Title

Imaging protective mast cells in living mice during severe contact hypersensitivity.

Laurent L. Reber[1,2], Riccardo Sibilano[2,3,*], Philipp Starkl[2,4,*], Axel Roers[5], Michele A. Grimbaldeston[6], Mindy Tsai[2,3], Nicolas Gaudenzio[2,3,#] & Stephen J. Galli[2,3,7,#].

[1] Department of Immunology, Unit of Antibodies in Therapy and Pathology, Institut Pasteur, Paris, France; INSERM, U1222, Paris, France.

[2] Department of Pathology, Stanford University School of Medicine, Stanford, CA 94305, USA.

[3] Sean N. Parker Center for Allergy and Asthma Research, Stanford University School of Medicine, CA 94305, USA.

[4] CeMM Research Center for Molecular Medicine of the Austrian Academy of Sciences, and Department of Medicine I, Medical University of Vienna, 1090, Vienna, Austria.

[5] Institute for Immunology, University of Technology Dresden, Medical Faculty Carl-Gustav Carus, 01307 Dresden, Germany.

[6] OMNI-Biomarker Development, Genentech Inc., South San Francisco, California 94080, USA

[7] Department of Microbiology & Immunology Stanford University School of Medicine, Stanford, CA 94305, USA

[*] and [#] Equal contribution; correspondence should be addressed to:

Nicolas Gaudenzio

269 Campus Drive, Room 3255b

Stanford, CA 94305-5176, USA

Telephone: (650) 736-6014

Email: ngaudenz@stanford.edu

or

Stephen J. Galli

269 Campus Drive, Room 3255b

Stanford, CA 94305-5176, USA

Telephone: (650) 736-6014

Email: sgalli@stanford.edu

Supplemental methods

Passive cutaneous anaphylaxis (PCA) model.

The left and right ear pinnae of mice were sensitized by means of an intradermal (i.d.) injection with mouse DNP-specific IgE (clone ε-26) (1) (20 ng in 20 μl PBS) or received an i.d. injection of 20 μl PBS (control), respectively. 16 h later, mice were injected i.p. with DNP-HSA (500 μg in 200 μl) to induce IgE-dependent cutaneous anaphylaxis. Some mice were injected i.p. with (200 μl) PBS as a control to assess the extent to which the observed inflammation was due to the sensitization with IgE antibodies. Ear thickness was measured before and at several intervals after challenge with a micrometer (Ozaki MFG). Toluidine blue and hematoxylin and eosin staining (H&E) of histological sections of ear pinnae, were performed as previously described (1).

Histology and quantification of mast cells, granulocytes, and epidermal thickness.

Mice were killed by CO_2 inhalation and samples of ear pinnae were fixed in 10% (vol/vol) buffered formalin and were embedded in paraffin (ensuring a cross-sectional orientation), and then sections 4 μm in thickness were cut. Ear sections were stained with 0.1% (vol/vol) toluidine blue, pH 1, for the detection of MCs, or with hematoxylin and eosin (H&E) for the detection of leukocytes. Ear pinna MCs were counted in 10 consecutive fixed fields, with a 20 x microscope objective (final magnification, x 100). Ear pinna leukocytes in the dermis between the epidermis and cartilage were counted in ten random fixed fields, under oil immersion with a 100 x microscope objective (final magnification, x 1,000). For quantification of epidermal thickness, images of 8 consecutive microscopic fields of toluidine blue–stained cross-sections of ear skin from each mouse, perpendicular to the epidermis, were obtained with a 40 x microscope objective (final magnification, x 200). For each image, eight randomly selected measurements of the distance between the stratum corneum and the bottom of the basal layer were recorded.

Two-photon microscopy.

Intravital analysis Av.SRho, Mcpt5-YEFP or IL-10-GFP staining in tissue.

8 μg of Av.SRho in 20 μl of PBS were injected i.d. into the ear pinna of the different mice described in **Figures 1 and 3 and Supplementary Figure 4**. 1 week later, mice were placed under the two-photon microscope, anesthesia was maintained by a mixture of Isoflurane/O_2 and the animal's ear pinna was kept at 36°C using a heating pad system. The fluorescence corresponding to Av.SRho$^+$ granule structures or EYFP$^+$ dermal MCs or IL-10-GFP were measured using a Prairie Ultima IV two-photon microscope (Spectra Physics Mai Tai HP Ti:sapphire laser, tunable from 690 to 1040 nm). Images were acquired in 3-D up to 30-50 μm depth, with 20x Olympus XLUM Plan Fl N.A. 0.95 water-immersion objective and a software zoom setting of 1 or 3 (8 bits/pixel 1024x1024, scaling x= 0.228 μm, y= 0.228 μm, z= 0.5 μm). Modeling and analysis of fluorescent signals were performed using untreated image sequences, as previously described (2), using Imaris software (Bitplane) and Image J software version Fiji, respectively. For the experiments described in **Figure 3 and Supplementary Figure 4**, the fluorescence corresponding to Av.SRho$^+$ granule structures or EYFP$^+$ dermal MCs or IL-10-GFP were monitored in the same animals over time at the site of injury (longitudinal imaging) after DNFB-challenge.

Dynamic imaging of tissue mast cell degranulation and vascular permeability (**Figure 2**)*.*

8 μg of Av.SRho in 20 μl of PBS were injected i.d. into the ear pinna of *C57BL/6* wild type mice. 1 week later, the ear pinnae of *C57BL/6* wild type mice were sensitized by i.d. injection of 20 ng of mouse anti-DNP IgE (clone ε-26) (1) in 20 μl PBS. 16 hours later, mice were positioned under the two-photon microscope, anesthesia was maintained by a mixture of Isoflurane/O_2 and the animal's ear pinna was kept at 36°C using a heating pad system for 20 min. To visualize the flowing blood, mice received a retro-orbital injection of 5 mg of 70-kDa dextran-FITC in 200 μl of PBS, as previously reported (3, 4). To induce IgE-mediated systemic anaphylaxis, anti-DNP IgE-

sensitized mice received an i.p. injection of 500 μg of DNP-HSA in 200 μl PBS or 200 μl PBS (control). Directly after injection, the fluorescence corresponding to Av.SRho and dextran-FITC-label in the blood stream were recorded simultaneously using the same two photon microscope as described above. Images were acquired in 3-D up to 50-60 μm depth, with one 3-D images sequence per 1.52 min for 30 min, with 20x Olympus XLUM Plan Fl W. N/A95 w.d2.0 objective and electronic zoom 3 (8 bits/pixel 512x512, scaling x= 1.37 μm, y= 1.37 μm, z= 4 μm). The interstitial spaces were randomly circumscribed and changes in dextran-FITC MFI were measured. Data were presented as fold increase from basal MFI at t=0 on untreated image sequences using the Measurement function of Image J software version Fiji (3, 4).

Bone marrow-derived cultured MCs (BMCMCs) and β-hexosaminidase release.

BMCMCs were generated as previously described (2). Briefly, mouse femoral bone marrow cells were cultured in DMEM medium supplemented with 10% fetal calf serum (FCS), penicillin and streptomycin and 20% WEHI-3 cell-conditioned medium (as a source of IL-3) to generate bone marrow-derived cultured MCs (BMCMCs). Cells were cultured for 6 weeks, with medium changed twice a week until >95% were FcεRIα$^+$KIT$^+$ (assessed by flow cytometry; data not shown). For the experiments depicted in **Supplemental Figure 2C**, BMCMCs were incubated for 4 days with 10 μg/ml of Av.SRho (the time to observe homogenous incorporation of the probe into BMCMCs secretory granules *in vitro*) or PBS (control) in the culture media and β-hexosaminidase release assay was performed as previously described (5).

Confocal laser-scanning microscopy.

Tissue analysis of KIT expression (**Supplemental Figure 1A**).

8 μg of Av.SRho in 20 μl of PBS were injected i.d. into the ear pinna of *C57BL/6* wild type mice. 1 week later, the ear pinnae was excised and fixed in 4% paraformaldehyde over-night (ON). Ear pinnae was then washed twice in PBS, permeabilized ON in 0.1% (vol/vol) Triton X100 in PBS and incubated ON with anti-c-KIT-Alexa fluor 647 antibody (1/100 in PBS; clone 2B8; Biolegend). Ear pinnae was then washed twice in PBS and mounted between slide and coverslip. Fluorescence was recorded in 3-D using a Zeiss LSM780 Meta inverted confocal laser-scanning microscope, 20x/0.8 WD=0.55 M27 objective and electronic zoom 1 (8 bits/pixel 8 bits/pixel 1024x1024, scaling x= 0.224 μm, y= 0.224 μm, z= 0.5 μm). Untreated 3-D images were analyzed using Imaris software (Bitplane).

In vitro monitoring of Av.SRho incorporation in BMCMCs (**Supplemental Figure 1C**).

5.10^4 BMCMCs were placed into poly-D-Lysine-coated (5 μg/ml in water) Nunc Lab-Tek 1.0 borosilicate cover glass system 8 chambers in culture medium supplemented with 10 μg/ml of Av.SRho. Av.SRho fluorescence intensity and location was recorded each day for 4 days in a controlled atmosphere (using a Zeiss stage-top incubation system with objective heater, 37°C and 5% humidified CO_2) using a Zeiss LSM780 Meta inverted confocal laser-scanning microscope, 37°C heated 63x/1.40 Oil DIC M27 objective and electronic zoom 3 (dimension x:512 y:512, scaling x= 0.264 μm and y= 0.264 μm). Untreated images were analyzed using Image J software version Fiji.

Supplemental Figures and Legends

Supplemental Figure 1

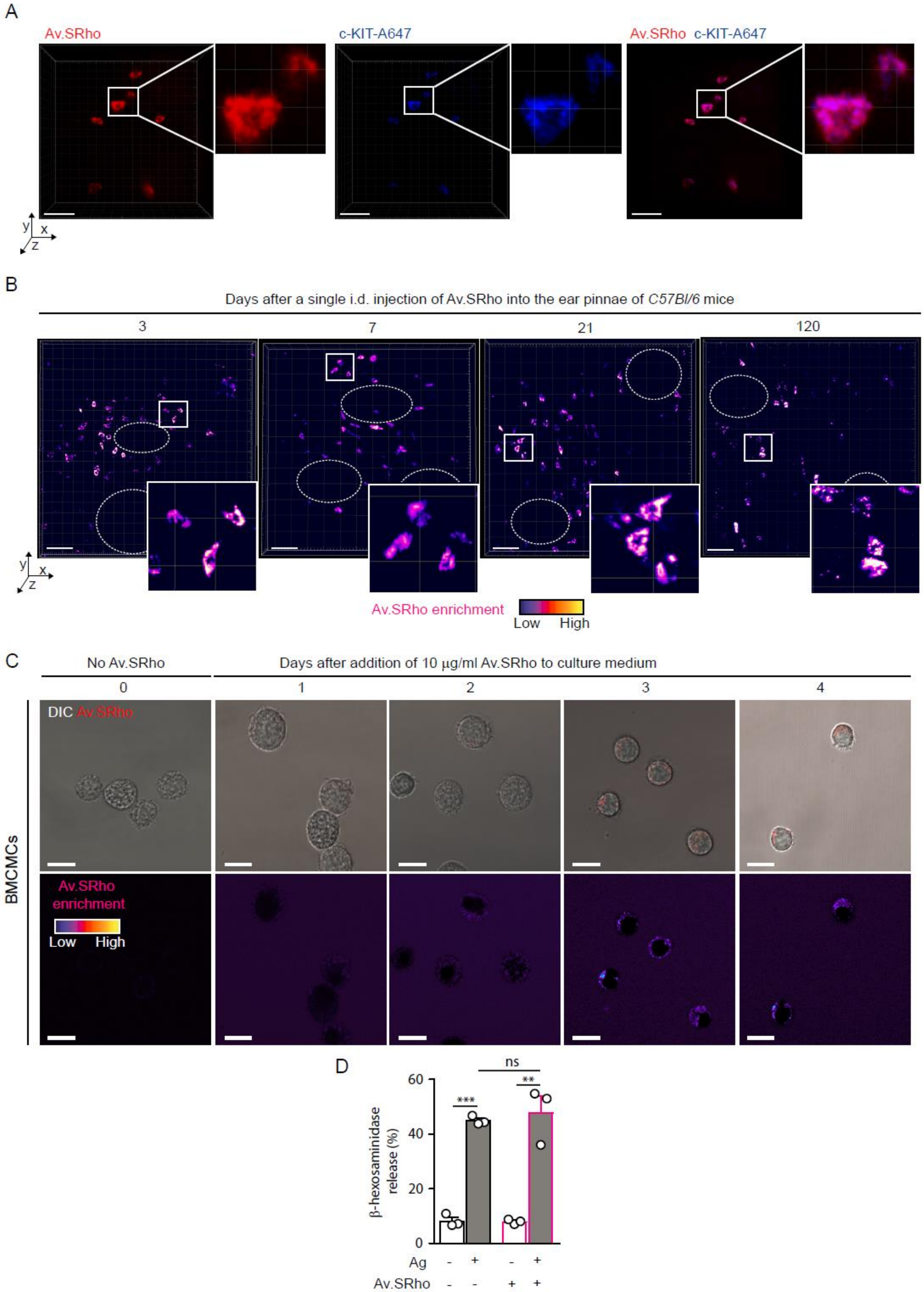

Supplemental Figure 1. A single injection of fluorochrome-labeled avidin enables long-term labeling of dermal mast cell *in vivo* and does not interfere with β-hexosaminidase release *in vitro*. (**A**) Representative confocal microscopy 3-D photographs of whole mounted Av.SRho (red)-injected ear pinnae that were also stained with Alexa647-labbeled anti-c-KIT antibody (blue). Bar = 50 μm. (**B**) Representative longitudinal two photon monitoring of ear pinnae in the same living mice at days 3, 7, 21 and 120 after i.d. injection of Av.SRho (pseudocolor scale). Bar = 100 μm. For **A** and **B**: Data (n = 3 mice per group) are pooled from the 3 experiments performed (each done with one mouse per group), each of which gave similar results. (**C**) Monitoring of Av.SRho (pseudocolor scale) incorporation into BMCMCs using confocal microscopy, at days 1, 2, 3 or 4 after addition of 10 μg/ml of Av.SRho to the culture medium. Bar = 30 μm. (**D**) Percentage of β-hexosaminidase release in BMCMCs 4 days after addition of 10 μg/ml of Av.SRho or PBS (control) to the culture medium. Mean ± SEM; two-tailed, unpaired *t* test; **P<.01; ***P<.001 and ns = not significant. Each dot represents from the result of 1 experiment. Data are pooled from the 3 independent experiments performed, each of which gave similar results.

Supplemental Figure 2

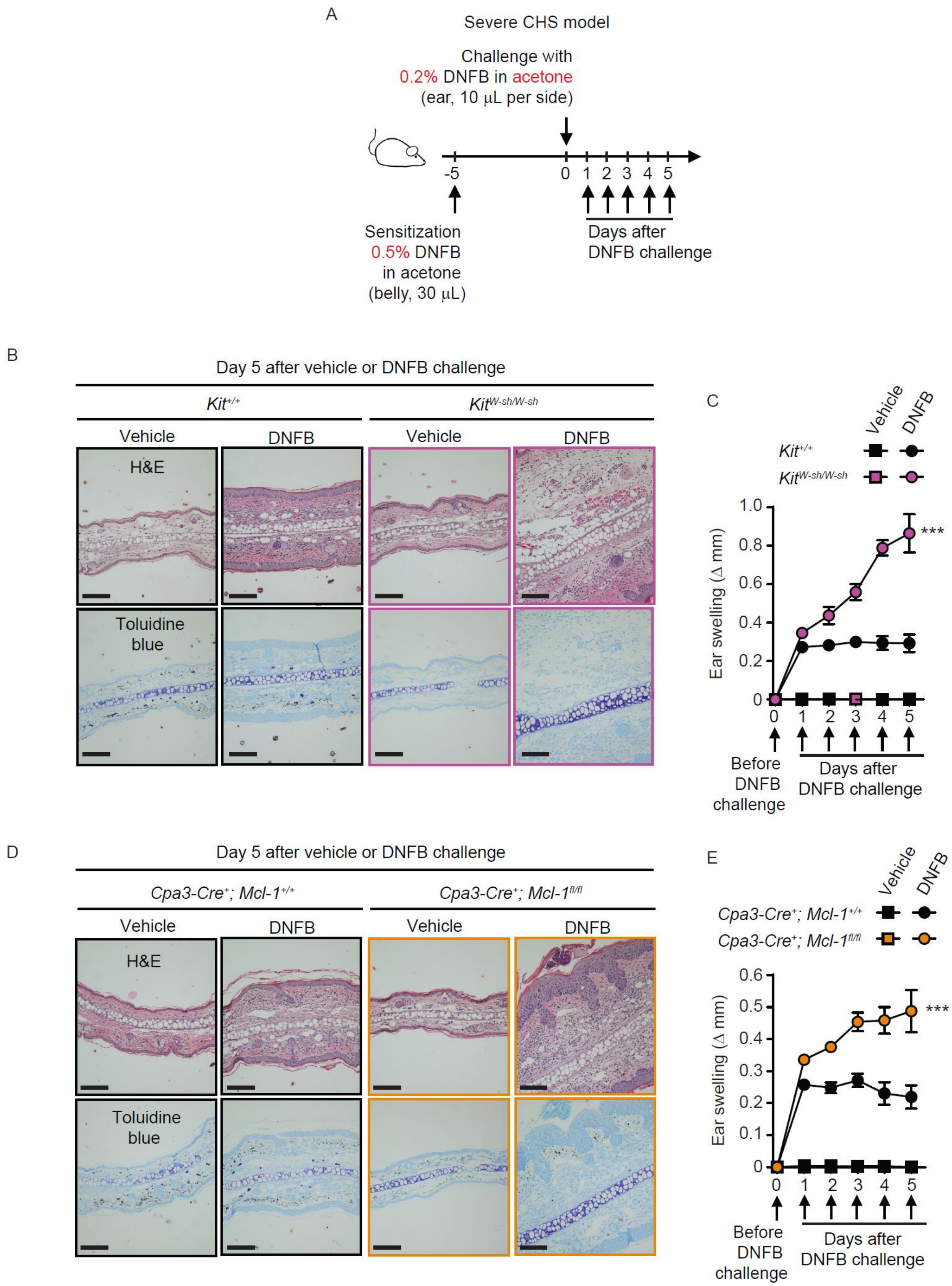

Supplemental Figure 2. *Kit*-dependent and *Kit*-independent MC-deficient mice exhibit increased inflammation and epidermal hyperplasia in a model of severe CHS. (**A**) Protocol to induce a severe CHS reaction. (**B**) Photomicrographs of representative H&E (upper panel) and TB (lower panel) stained sections of ear pinnae of mice sacrificed 5 days after challenge. (**C**) Changes (∆) in ear thickness over time after challenge with vehicle (squares) or DNFB (circles) in $Kit^{W\text{-}Sh/W\text{-}Sh}$ (MC-deficient, purple) or $Kit^{+/+}$ (MC-sufficient, black) mice. (**D**-**E**) Same as described in **B** and **C** but in *Cpa3-cre*$^{+}$*; Mcl-1*$^{fl/fl}$ (MC-deficient, orange) or *Cpa3-cre*$^{-}$*; Mcl-1*$^{fl/fl}$ (MC-sufficient, black) mice. Mean ± SEM; two-way ANOVA, ***P<.001. Data (n = 7-11 mice per group) are pooled from the 3 independent experiments performed (each done with n = 2-4 mice per group), each of which gave similar results.

Supplemental Figure 3

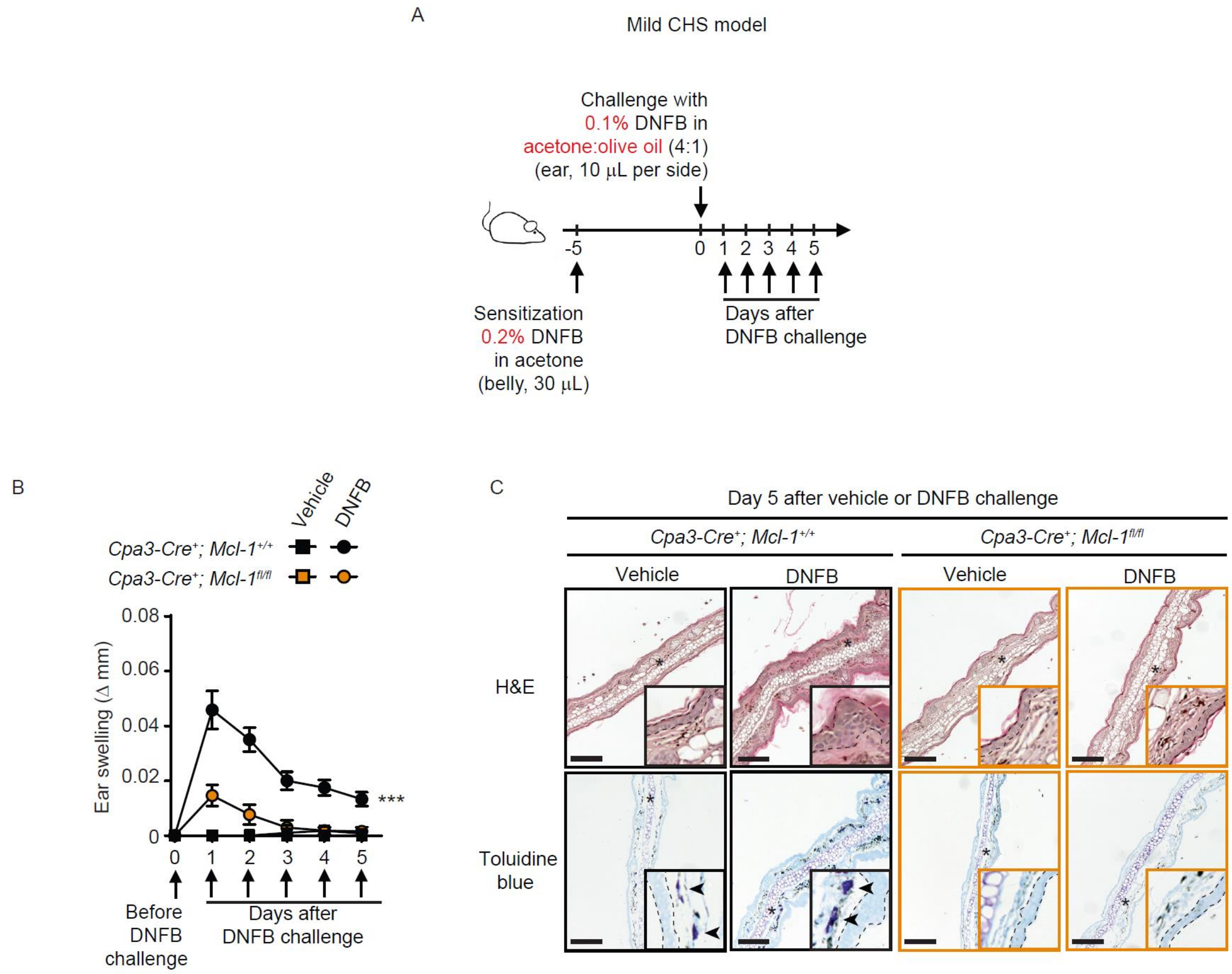

Supplemental Figure 3. *Kit*-independent MC-deficient mice exhibit reduced inflammation and epidermal hyperplasia in a model of mild CHS. (**A**) Protocol to induce a mild CHS reaction. (**B**) Changes (Δ) in ear thickness over time after challenge with vehicle (squares) or DNFB (circles) in *Cpa3-cre*$^{+}$*; Mcl-1*$^{fl/fl}$ (MC-deficient, purple) or *Cpa3-cre*$^{-}$*; Mcl-1*$^{fl/fl}$ (MC-sufficient, black) mice. (**C**) Photomicrographs of representative H&E (upper panel) and TB (lower panel) stained sections of ear pinnae of mice sacrificed 5 days after challenge. Mean ± SEM; two-way ANOVA, ***P<.001. Data (n = 12-13 mice per group) are pooled from the 3 independent experiments performed (each done with n = 4-5 mice per group), each of which gave similar results.

Supplementary Figure 4

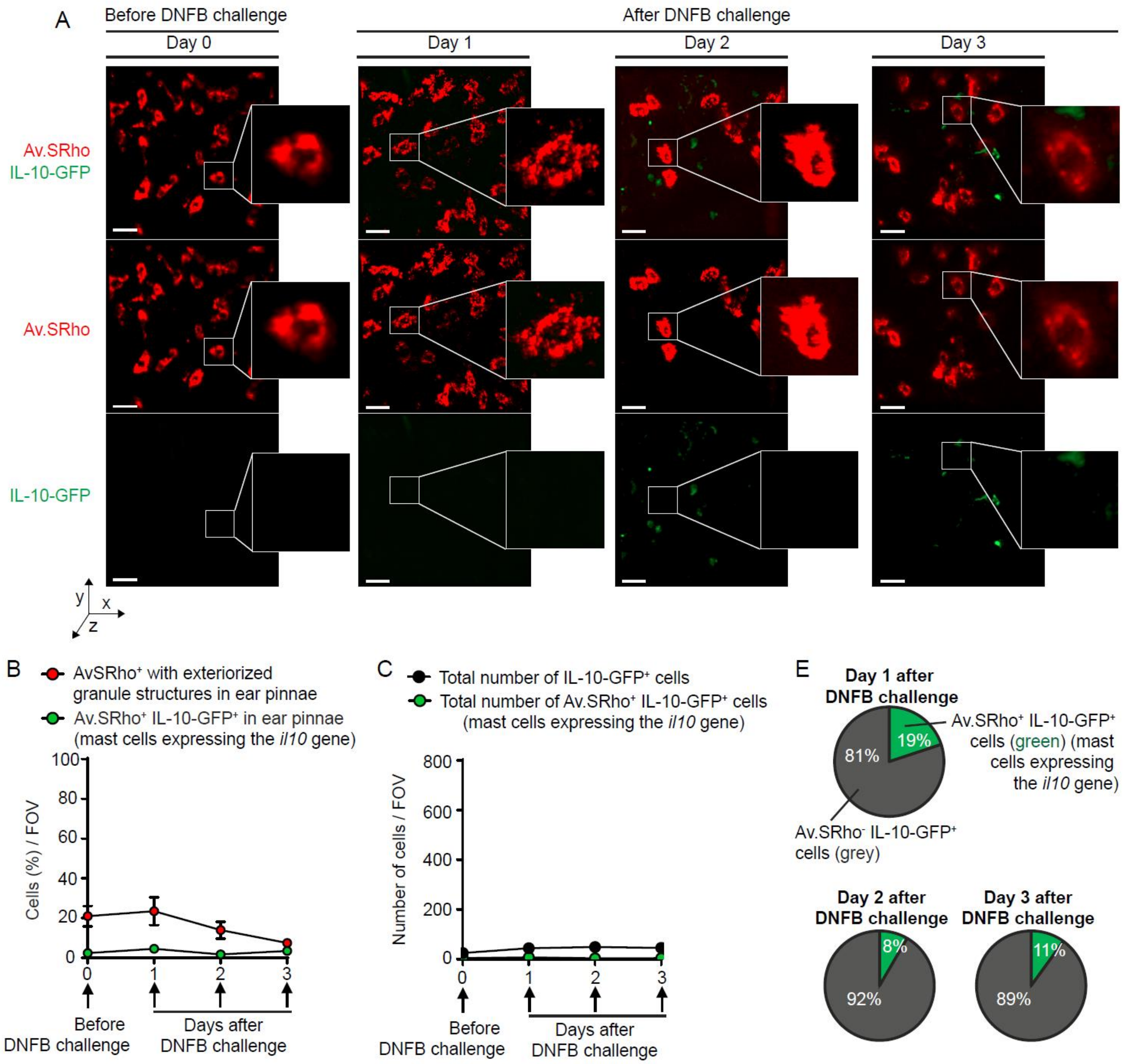

Supplementary Figure 4. Longitudinal imaging of MC degranulation and *il10* gene activation in a model of mild CHS. 5 μg of Av.SRho was injected i.d. into the ear pinna of mice. 1 week later, the mice were treated as depicted in **Supplemental Figure 3A** to induce a mild DNFB-induced CHS reaction. (**A**) Longitudinal monitoring of both the release of dermal MC Av.SRho^{+} granules and activation of *il10* gene transcription (IL-10-GFP, as detected by emission of GFP fluorescent signal) at the site of CHS using intravital two-photon microscopy.

Representative 3-D photographs of the ear pinna before DNFB challenge or at day 1, 2 or 3 after DNFB challenge; upper panel: merged fluorescence of Av.SRho (red) and IL-10-GFP (green); middle panel: Av.SRho (red) fluorescence; lower panel: IL-10-GFP (green) fluorescence. White lines identify the magnified areas. Bars = 20 μm. (**B**) Percentage of Av.SRho^{+} cells with exteriorized granule structures (i.e., degranulated dermal MCs, red circles) and of Av.SRho^{+} IL-10-GFP^{+} cells (i.e., representing MCs expressing the *il10* gene, green circles) per FOV in ear pinnae. (**C)** Total number of Av.SRho^{+} IL-10-GFP^{+} cells (MCs expressing the *il10* gene, green circles) per FOV in ear pinnae and total number of IL-10-GFP^{+} cells in ear pinnae (black circles). (**D**) Percentage of Av.SRho^{+} IL-10-GFP^{+} cells (i.e., representing MCs expressing the *il10* gene, green) and of Av.SRho^{-} IL-10-GFP^{+} cells (i.e., representing other cell types expressing the *il10* gene, grey) among total IL-10-GFP^{+} cells in ear pinnae per FOV. Mean ± SEM; data (n = 3 per group) are pooled from the 3 independent experiments performed (each done with one mouse per group), each of which gave similar results.

Supplemental Video 1. Mast cell secretory granule changes and plasma extravasation dynamics after vehicle injection *in vivo*. 5 μg of Av.SRho (red) were injected i.d. into the ear pinnae of *C57BL/6* wild type mice. 1 week later, the mice were sensitized by i.d. injection into the ear pinna of 20 ng of mouse anti-DNP IgE (or received PBS i.d. as a control). 16 h later, we retro-orbitally injected 250 μg of 70-kDa dextran-FITC (green) and the anesthetized mice were positioned under the two-photon microscope. Mice were injected i.p. with vehicle. Image sequences were acquired in 3-D at a rate of one picture per min over 30 min using a two-photon microscope. Collagen structures are shown in blue. The video shows 3 examples of Av.SRho^{+} MCs close to a dextran-FITC^{+} blood vessel. Bars = 10 μm. We noted no differences in findings in ears injected i.d. with anti-DNP IgE or PBS.

Supplemental Video 2. Mast cell secretory granule changes and plasma extravasation dynamics during IgE-dependent reactions *in vivo*. 5 μg of Av.SRho (red) are injected i.d. into the ear pinnae of *C57BL/6* wild type mice. 1 week later the mice were sensitized or not by i.d. injection into the ear pinna of 20 ng of mouse anti-DNP IgE. 16 h later, we retro-orbitally injected 250 μg of 70-kDa dextran-FITC (green) and the anesthetized mice were positioned under the two-photon microscope. Mice were injected i.p. with 500 μg of DNP-HSA. Image sequences were acquired in 3-D at a rate of one picture per min over 30 min using a two-photon microscope. Collagen structures are shown in blue. The video shows 3 examples of Av.SRho$^+$ MCs close to a dextran-FITC$^+$ blood vessel. Bars = 15 μm for example #1 and 10 μm for examples #2 and 3.

Supplemental references

1. Schafer B, Piliponsky AM, Oka T, Song CH, Gerard NP, Gerard C, et al. Mast cell anaphylatoxin receptor expression can enhance IgE-dependent skin inflammation in mice. *J Allergy Clin Immunol.* 2012;131(2):m541-8.
2. Gaudenzio N, Sibilano R, Starkl P, Tsai M, Galli SJ, and Reber LL. Analyzing the Functions of Mast Cells In Vivo Using 'Mast Cell Knock-in' Mice. *Journal of visualized experiments : JoVE.* 2015(99):e52753.
3. Egawa G, Nakamizo S, Natsuaki Y, Doi H, Miyachi Y, and Kabashima K. Intravital analysis of vascular permeability in mice using two-photon microscopy. *Scientific reports.* 2013;3:1932.
4. Gaudenzio N, Sibilano R, Marichal T, Starkl P, Reber LL, Cenac N, et al. Different activation signals induce distinct mast cell degranulation strategies. *J Clin Invest.* 2016.
5. Akahoshi M, Song CH, Piliponsky AM, Metz M, Guzzetta A, Abrink M, et al. Mast cell chymase reduces the toxicity of Gila monster venom, scorpion venom, and vasoactive intestinal polypeptide in mice. *J Clin Invest.* 2011;121(10):4180-91.